Physics Letters B 683 (2010) 248–254

Contents lists available at ScienceDirect

Physics Letters B

www.elsevier.com/locate/physletb

Enhanced anti-deuteron Dark Matter signal and the implications of PAMELA

Mario Kadastik [a,*], Martti Raidal [a], Alessandro Strumia [b,c]

[a] NICPB, Ravala 10, 10143 Tallinn, Estonia
[b] Dipartimento di Fisica dell'Università di Pisa and INFN, Italy
[c] CERN, PH-TH, CH-1211, Geneva 23, Switzerland

ARTICLE INFO

Article history:
Received 21 August 2009
Received in revised form 4 December 2009
Accepted 4 December 2009
Available online 11 December 2009
Editor: A. Ringwald

ABSTRACT

We show that the jet structure of DM annihilation or decay products enhances the $\bar{d}$ production rate by orders of magnitude compared to the previous computations done assuming a spherically symmetric coalescence model. In particular, in the limit of heavy DM, $M \gg m_p$, we get a constant rather than $1/M^2$ suppressed $\bar{d}$ production rate. Therefore, a detectable $\bar{d}$ signal is compatible with the lack of an excess in the $\bar{p}$ PAMELA flux. Most importantly, cosmic $\bar{d}$ searches become sensitive to the annihilations or decays of heavy DM, suggesting to extend the experimental $\bar{d}$ searches above the $\mathcal{O}(1)$ GeV scale.

1. Introduction

The cosmological DM abundance is naturally produced in thermal freeze-out if Dark Matter (DM) has weak interactions and a TeV-scale mass M, that in appropriate models can be lowered down to the weak scale, 100 GeV. This scenario can be tested searching for DM annihilation (or decay) products in cosmic rays. In view of astrophysical backgrounds, a particularly sensitive signal is an excess in cosmic-ray anti-particles: positrons, anti-protons $\bar{p}$ and anti-deuterium $\bar{d}$. According to the coalescence prescription [1], a $\bar{d}$ is formed when DM produces a $\bar{p}$ and a $\bar{n}$ with momentum difference below $p_0 \approx 160$ MeV. The standard formula for the $\bar{d}$ spectrum, obtained under the assumption of *spherical symmetry* of the events, in terms of the anti-nucleon ($\bar{p}$ plus $\bar{n}$) energy spectrum per annihilation, dN_N/dT, is [2–4,6,7]

$$\frac{dN_{\bar{d}}}{dT_{\bar{d}}} = \frac{p_0^3}{3k_{\bar{d}} m_p} \left(\frac{1}{2} \frac{dN_N}{dT} \right)^2_{T=T_d/2}, \tag{1}$$

where the kinetic energies $T = E - m$ are $T_p = T_n = T_d/2$, $m_p = m_n = m_d/2$ and $k_{\bar{d}} = \sqrt{T_{\bar{d}}^2 + 2m_d T_{\bar{d}}}$. Eq. (1) implies a $\bar{d}$ yield suppressed by $1/M^2$ for large M. This result is qualitatively wrong. Increasing M just increases the boost of the primary DM annihilation products, giving rise, due to Lorentz symmetry, to an essentially constant $\bar{d}$ production rate with energy roughly proportional to M. The reason for this fundamental discrepancy is caused by the fact that the spherical approximation misses the jet structure of the DM annihilation products.

In this Letter we show that for $M \gg m_p$ the angular proximity of the produced $\bar{p}$, $\bar{n}$ enhances the $\bar{d}$ yield, possibly by orders of magnitude. We critically compare the standard spherical approximation results with our Monte Carlo approach to $\bar{d}$ production, presenting the $\bar{d}$ energy spectra for the various DM annihilation or decay channels into W^+W^-, ZZ, $q\bar{q}$, $b\bar{b}$, $t\bar{t}$, hh and comment on the astrophysical $\bar{d}$ background produced mostly in cosmic ray pp and $p\bar{p}$ collisions. We propagate $\bar{d}$ in the Milky Way, studying the phenomenology and the prospects for DM produced $\bar{d}$ searches at AMS-2, in the light of the PAMELA $\bar{p}$ observations. We find that the $\bar{d}$ signal below 1 GeV is strongly enhanced increasing the chances of $\bar{d}$ detection at AMS-2 even for the standard thermal DM annihilation cross section. This result is consistent with the lack of $\bar{p}/p$ excess in PAMELA. Due to the qualitatively different large M behavior of the production rate, our result drastically enhance the $\bar{d}$ production at high energies. Therefore the cosmic ray $\bar{d}$ flux produced in heavy DM annihilations or decays exceeds the estimated background, and AMS-2 and future $\bar{d}$ experiments become sensitive to DM if they extend their sensitivity to $\bar{d}$ above 1 GeV.

2. Spherical-cow vs Monte Carlo

$\bar{d}$ is formed via $\bar{p}\bar{n} \to \bar{d}\gamma$, that has a large cross section due to the small binding energy of $\bar{d}$, which therefore has a spatially extended wave-function or equivalently a strongly peaked wavefunction $\psi(\Delta k) \equiv \langle \bar{d} | \bar{p}\bar{n} \rangle$ in momentum space. Here $\bar{d}$ has momentum k_d and energy E_d and Δk is the relativistically invariant relative momentum between $\bar{p}$ (with momentum $\vec{k}_p$ and energy E_p) and $\bar{n}$ (with momentum $\vec{k}_n$ and energy E_n):

$$\Delta k^2 = |\vec{k}_p - \vec{k}_n|^2 - (E_p - E_n)^2 + (m_n - m_p)^2, \tag{2}$$

* Corresponding author.
E-mail address: mario.kadastik@cern.ch (M. Kadastik).

0370-2693
doi:10.1016/j.physletb.2009.12.005

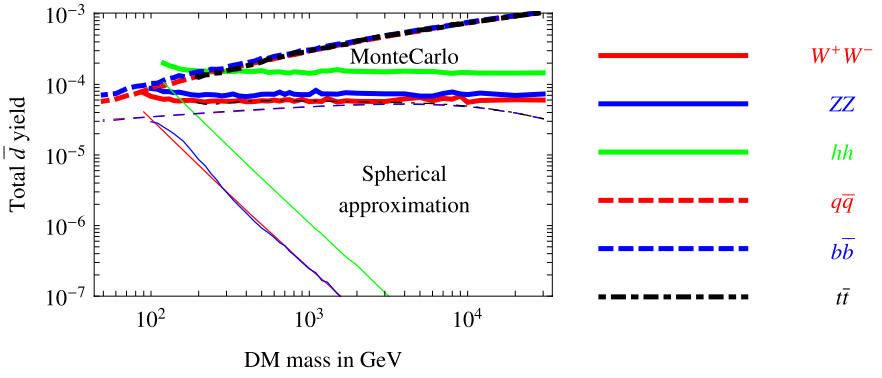

Fig. 1. Total $\bar{d}$ yield per DM annihilation as a function of the DM mass. The thick upper lines present the Monte Carlo result, and the lower thin lines are the spherical approximation. The annihilation modes are into W^+W^- (red), ZZ (blue), hh (green) $t\bar{t}$ (black dot-dashed), $b\bar{b}$ (blue dashed), light quarks $q\bar{q}$ (red dashed). (For interpretation of the references to color in this figure legend, the reader is referred to the web version of this Letter.)

where we can neglect $m_p - m_n = 1.29$ MeV. The amplitude for $\bar{d}$ production in DM annihilations, $\mathrm{DM\,DM} \to \bar{d}$, can be computed as

$$\langle \bar{d}|\mathrm{DM\,DM}\rangle = \sum_{\bar{p},\bar{n}} \langle \bar{d}|\bar{p}\bar{n}\rangle \langle \bar{p}\bar{n}|\mathrm{DM\,DM}\rangle, \tag{3}$$

giving the 'coalescence approximation' [1]: the probability $|\langle \bar{d}|\bar{p}\bar{n}\rangle|^2$ that a $\bar{p}$ and a $\bar{n}$ coalesce to form a $\bar{d}$ is approximated as a narrow step function $\Theta(\Delta k - p_0)$, that drops from unity to zero if Δk is larger than p_0. Here p_0 is a constant (to be extracted from data later) that can be estimated as $p_0 \sim \sqrt{m_d B_d} \sim 60$ MeV assuming that $\bar{d}$ production happens until the relative $\bar{p}$, $\bar{n}$ kinetic energy is smaller than the deuteron binding energy $B_d = 2.2$ MeV. The total $\bar{d}$ yield therefore is

$$\begin{aligned} N_d &= \int dN_p\, dN_n\, \Theta\big(\Delta k^2 - p_0^2\big) \\ &= \int d^3k_p\, d^3k_n \frac{dN_p\, dN_n}{d^3k_p\, d^3k_n} \Theta\big(\Delta k^2 - p_0^2\big). \end{aligned} \tag{4}$$

In the non-relativistic limit $k_{p,n} \ll m_{p,n}$ and for small p_0 the region that satisfies $\Delta k < p_0$ at fixed $\vec{k}_n$ is a sphere in $\vec{k}_p$ centered on $\vec{k}_n$ with radius p_0 and volume $4\pi p_0^3/3$. In general the sphere gets dilatated along the direction $\vec{k}_p \approx \vec{k}_n$ by a relativistic Lorentz factor $\gamma_p \approx \gamma_n \approx \gamma_d$. Multiplying Eq. (4) times $1 = \int d^3k_d\, \delta(\vec{k}_d - \vec{k}_p - \vec{k}_n)$ we finally get, in the limit of small $p_0 \ll M/\gamma_{p,n}$, the $\bar{d}$ momentum distribution:

$$\gamma_d \frac{dN_d}{d^3k_d} = \frac{1}{8}\frac{4\pi p_0^3}{3} \gamma_n \gamma_p \frac{dN_p\, dN_n}{d^3k_p\, d^3k_n}, \tag{5}$$

where $\vec{k}_p = \vec{k}_n = \vec{k}_d/2$.[1] Eq. (5) is relativistically invariant as it contains the usual relativistic phase space $d^3k/2E = d^4k\delta(E^2 - k^2 - m^2)$.

2.1. The spherical approximation

Previous computations proceed assuming spherical symmetry, $d^3k = 4\pi k^2\, dk$, and uncorrelated $\bar{p}$, $\bar{n}$ distributions:

$$\frac{dN_p\, dN_n}{d^3k_p\, d^3k_n} = \frac{dN_p}{d^3k_p} \cdot \frac{dN_n}{d^3k_n} \quad \text{implying} \quad \frac{E}{m}\frac{dN}{d^3k} = \frac{1}{4\pi k m}\frac{dN}{dE}. \tag{6}$$

[1] The extra factor of 8 with respect to the equation used in papers [2–7] comes from $d^3k_d = 8d^3k_{p,n}$. In the final result this difference gets compensated by a value of p_0 twice larger than the one adopted in those papers. In our Monte Carlo computation of the coalescence condition $\Delta k < p_0$ it is important that we fix factors of 2 so that our p_0 really is the radius of the coalescence sphere.

Writing the result in terms of the adimensional $x_i = T_i/M$ (so that $0 \leqslant x_{d,p,n} < 1$ and $x_p = x_n = x_d/2$) one gets Eq. (1) i.e.

$$\frac{dN_d}{dx_d} = \frac{p_0^3}{3M^2 m_p} \frac{1}{\sqrt{x_d^2 + 4m_p x_d/M}} \frac{dN_p}{dx_p}\frac{dN_n}{dx_n}, \tag{7}$$

which is explicitly suppressed by $1/M^2$ for large DM mass M.

This is qualitatively wrong. Consider for example the $\mathrm{DM\,DM} \to W^+W^-$ annihilation mode. Increasing M increases the boost of each W, and thereby the boost of the anti-deuterons from W decay, but the $\bar{d}$ number stays fixed. Neglecting QED final state radiation (FSR), for $M \gg M_W$ one should get a constant, M-independent function for dN_d/dx_d. Obviously the problem is in the 'spherical-cow' approximation [8]. Due to the $W^\pm$ boost the events are highly non-spherical and SM particles are concentrated in two back-to-back jets, enhancing the probability of having $\bar{p}\bar{n}$ pairs with small momentum difference $\Delta k < p_0$. A similar argument applies to DM annihilations or decays into colored particles, such as $q\bar{q}$. Hadronization leads to QCD jets, rather than to spherical events. Thereby the spherical approximation can grossly underestimate the $\bar{d}$ production.

Going to less relevant aspects that control order one factors, the analytic spherical approximation can also over-estimate the $\bar{d}$ yield, by neglecting anti-correlations between $\bar{n}$ and $\bar{p}$ or the fact that no $\bar{d}$ is obtained if only one anti-nucleon is present per event. As an example, we consider again the W^+W^- mode: within the spherical approximation a $\bar{d}$ can form coalescing a $\bar{p}$ from W^- with a $\bar{n}$ from W^+, but this process is highly suppressed because the W^+ and W^- go back to back.

2.2. The Monte Carlo approach

In order to take into account the jet structure of the events and the correlations between the $\bar{p}, \bar{n}$ momenta we compute the $\bar{d}$ spectrum by searching *event-by-event* for the $\bar{n}, \bar{p}$ pair(s) which have relativistically invariant momentum difference Δk smaller than p_0. We verified that the spherical uncorrelated approximation of Eq. (7) is reproduced if we first merge many events, and later coalesce $\bar{p}$ with $\bar{n}$ without imposing that they come from the same event.

Various experiments extracted compatible values of p_0 from data about $\bar{d}$ production in hadronic and e^+e^- collisions. Presumably these studies adopted the 'spherical-cow' approximation rather than performing a Monte Carlo computation. Giving the relatively low energies involved this should not make a large difference; anyhow we here prefer to directly extract p_0 from the ALEPH data [9]: one hadronic Z decay at rest gives rise to $(5.9 \pm$

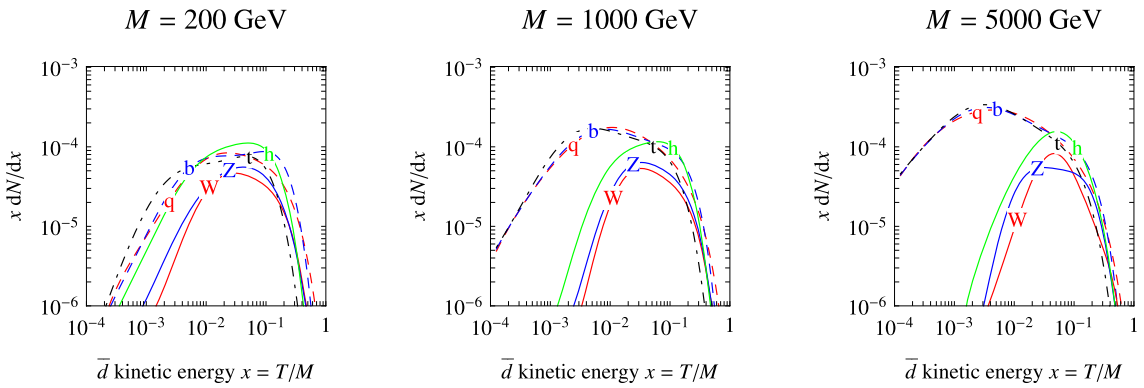

Fig. 2. Monte Carlo results for the $\bar{d}$ spectra $x \cdot dN/dx$ produced per DM annihilation into W^+W^-, ZZ, hh $t\bar{t}$, $b\bar{b}$, $q\bar{q}$. We assumed the DM mass $M = 200$ GeV (1 TeV) [5 TeV] in the left (middle) [right] panel. The notation is the same as in Fig. 1.

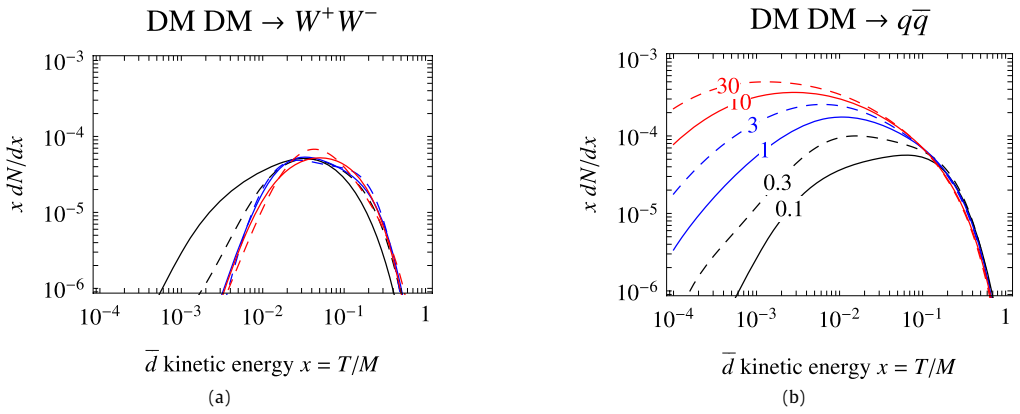

Fig. 3. Monte Carlo results for the $\bar{d}$ spectra per DM annihilation, $x \cdot dN/dx$ for $p_0 = 160$ MeV. We consider DM masses $M = 0.1, 1, 10$ TeV (black, blue, red continuous curves) and $M = 0.3, 3, 30$ TeV (black, blue, red dashed curves) and the indicated DM annihilation modes. (For interpretation of the references to color in this figure legend, the reader is referred to the web version of this Letter.)

$1.9) \times 10^{-6}$ $\bar{d}$ in the momentum range 0.62 GeV $< k_d <$ 1.03 GeV and angular range $|\cos\theta| < 0.95$. According to our Monte Carlo computation, this translates into $p_0 = 162 \pm 17$ MeV. Should p_0 have a value different from the $p_0 = 160$ MeV adopted here for both the DM signal and the astrophysical background (as computed in [2,4]) the $\bar{d}$ energy spectra get rescaled roughly by an overall $(p_0/160\ \text{MeV})^3$ factor.

We performed a Monte Carlo study by generating a huge number of events (up to 10^7 per DM DM annihilation, and up to 10^9 events when studying pp and $p\bar{p}$ collisions) with Pythia 8 [10], directly implementing the condition $\Delta k < p_0 = 160$ MeV for $\bar{d}$ production. Such computing-power demanding results have been obtained using the EU Baltic Grid facilities [11].

Fig. 1 shows the total number of $\bar{d}$ produced per DM annihilation as function of the DM mass for various annihilation modes, comparing our Monte Carlo result with the spherical approximation, which can under-estimate the $\bar{d}$ yield by various orders of magnitude. The same $p_0 = 160$ MeV is assumed in both cases.

Fig. 2 shows our Monte Carlo results for the $\bar{d}$ spectra computed for three values of the annihilating DM mass M. The same spectra also hold for decaying DM, after replacing $M_{\text{ann}} \to M_{\text{dec}}/2$. As we expected, the result has only a minor dependence on M and is thereby qualitatively different from the 'spherical-cow' approximation that would give a $1/M^2$ suppression. There are three classes of qualitatively different cases: DM annihilations i) into W, Z, h (we assume a Higgs mass $m_h = 120$ GeV); ii) into quarks q, b, t or iii) into leptons. The latter case gives no $\bar{d}$. To compare the former two cases that give $\bar{d}$, we focus on i) DM DM $\to W^+W^-$ and ii) DM DM $\to q\bar{q}$, and show the $\bar{d}$ spectra in Fig. 3a and b, respectively, for various values of the DM mass M. In the W^+W^- case the $\bar{d}$ spectrum only mildly depends on the DM mass. Neglecting FSR, all $\bar{d}$ should have $x > m_d/M_W = 0.05$; the small $\bar{d}$ flux at smaller x is due to electroweak FSR. In the $q\bar{q}$ case the $\bar{d}$ spectrum at smaller x increases with M rather than being suppressed as $1/M^2$. This is due to QCD FSR that roughly scales as $\alpha_3 \ln(M/m_p)$.

The Monte Carlo results differ both qualitatively and quantitatively from the previous studies of the $\bar{d}$ spectra in DM annihilations or decays. To draw conclusions about the detectability of the signal, we also need to study possible changes in the astrophysical $\bar{d}$ background, mainly generated by collisions of cosmic-ray p with energy E_p on p at rest. In view of the kinematical threshold for $\bar{d}$ production ($E_p \gtrsim 30$ GeV) and of the energy spectrum of cosmic protons (roughly proportional to E_p^{-3}), $\bar{d}$ production is dominated by $E_p \sim 60$ GeV, in the range of validity of the parton model in Pythia. Our semi-quantitative results for the $\bar{d}$ background suggest a reasonable agreement with the spectra of [2,4]. This is an expected result because the center of mass energy in cosmic pp collisions is small and, in this case, the uncorrelated spherical approximation is expected to work reasonably well. However this issue needs to be precisely investigated.

Some remarks are in order. First, we computed p, n allowing all other hadrons to decay despite that the life-time of some strange baryons, such as the $\Xi = uss$, is longer than the size of deuterium. This effect should already have been taken into account when extracting the value of p_0 from high-energy experimental data from its definition of Eq. (5). Second, DM in general annihilates into various primary channels k. According to Eq. (1) one should sum their

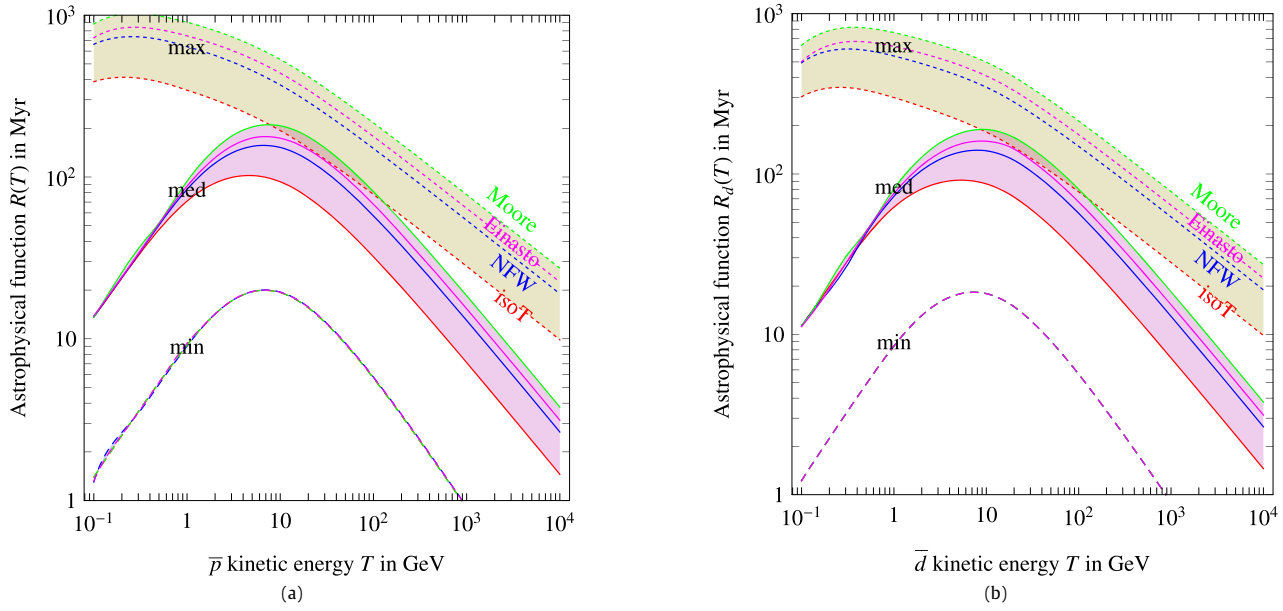

Fig. 4. The $\bar{p}$ (left) and $\bar{d}$ (right) astrophysical functions, $R(T)$ and $R_d(T)$ of Eq. (11), computed under different assumptions. In both cases, the dashed (solid) [dotted] bands assumes the min (med) [max] propagation configurations. Each band contains 4 lines, that correspond to the isothermal (red lower lines), NFW (blue middle lines), Einasto (magenta) and Moore (green upper lines) DM density profiles. (For interpretation of the references to color in this figure legend, the reader is referred to the web version of this Letter.)

contributions to the $\bar{p}$, $\bar{n}$ spectra rather than to the $\bar{d}$ spectrum, getting $(\sum_k dN^{(k)}/dx)^2 \neq \sum_k (dN^{(k)}/dx)^2$. Our Monte Carlo result instead amounts to sum incoherently over all primary annihilation channels k as well as all secondary and tertiary contributions in the decay chain.

3. Cosmological fluxes

To compute the $\bar{d}$ flux in the solar system we consider four possible Milky Way DM density profiles $\rho(r)$ [12]:

$$\frac{\rho(r)}{\rho_\odot} = \begin{cases} (1+r_\odot^2/r_s^2)/(1+r^2/r_s^2) \\ \quad \text{isothermal},\ r_s = 5\ \text{kpc}, \\ (r_\odot/r)(1+r_\odot/r_s)^2/(1+r/r_s)^2 \\ \quad \text{NFW},\ r_s = 20\ \text{kpc}, \\ (r_\odot/r)^{1.16}(1+r_\odot/r_s)^2/(1+r/r_s)^{1.84} \\ \quad \text{Moore},\ r_s = 30\ \text{kpc}, \\ \exp(-2[(r/r_s)^\alpha - (r_\odot/r_s)^\alpha]/\alpha) \\ \quad \text{Einasto},\ r_s = 20\ \text{kpc},\ \alpha = 0.17, \end{cases} \tag{8}$$

keeping fixed the local DM density $\rho(r = r_\odot) = \rho_\odot = 0.3\ \text{GeV/cm}^3$. Concerning diffusion of charged $\bar{d}$ in the galaxy, we approximate the diffusion region as a cylinder with height $2L$ centered on the galactic plane, a constant diffusion coefficient $K = K_0 E^\delta$ and a constant convective wind directed outward perpendicularly to the galactic plane. We consider the min, med, max propagation models [13] for $\bar{p}$, $\bar{d}$, which are characterized by the following astrophysical parameters,

Model	δ	K_0 in kpc^2/Myr	L in kpc	V_{conv} in km/s
min	0.85	0.0016	1	13.5
med	0.70	0.0112	4	12
max	0.46	0.0765	15	5

(9)

Finally, one must take into account annihilations of $\bar{d}$ on interstellar protons and helium in the galactic plane (with a thickness of $h = 0.1\ \text{kpc} \ll L$) with rate Γ_{ann} [2]. The solution to the diffusion equation for the energy spectrum of the $\bar{d}$ number density, f,

$$-K(T)\cdot\nabla^2 f + \frac{\partial}{\partial z}\big(\text{sign}(z) f V_{\text{conv}}\big) = Q - 2h\delta(z)\Gamma_{\text{ann}} f, \tag{10}$$

acquires a simple factorized form in the "no-tertiaries" approximation that we adopt. The $\bar{d}$ flux in the galactic medium around the solar system can be written as

$$\frac{d\Phi_{\bar{d}}}{dT} = \frac{v_{\bar{d}}}{4\pi} f = \frac{v_{\bar{d}}}{4\pi}\frac{\langle\sigma v\rangle}{2}\left(\frac{\rho_\odot}{M}\right)^2 R_d(T)\frac{dN_{\bar{d}}}{dT}, \tag{11}$$

fully analogous to the solution for the $\bar{p}$ flux in [14]. The function $dN_{\bar{d}}/dT$ contains the particle physics input and was computed in the previous section. The function $R_d(T)$ encodes the Milky Way astrophysics and is plotted in Fig. 4b for various halo and propagation models. It roughly is some average containment time in the diffusion cylinder, and we verified that $\bar{d}$ generated outside it provide a negligible extra contribution even in the min scenario, where most DM annihilations occur outside the diffusion cylinder: the probability of re-entering is sizable, but the probability of diffusing up to the solar system is small. Going from DM annihilations to DM decays with life-time τ one just needs to replace in Eq. (11) $\langle\sigma v\rangle\rho_\odot^2/2M^2$ with $\rho_\odot/M\tau$; we do not plot the corresponding $R_d(T)$ functions for DM decay as they essentially coincide with the R_d function for DM annihilations and the *isothermal* profile plotted in Fig. 4b. Indeed, for all the considered DM profiles, DM decays close to the galactic center do not significantly contribute to the $\bar{d}$ flux at Earth, as for DM annihilations with the quasi-constant isothermal density profile.

We notice that although $R_d(T)$ is significantly uncertain (especially below a few GeV), the ratio with the corresponding astrophysical function $R(T)$ for $\bar{p}$ is essentially fixed, so that the non-observation of a DM $\bar{p}$ excess puts robust bounds on the possible DM $\bar{d}$ flux. Indeed the $\bar{p}$ flux has been observed below 100 GeV by PAMELA [15] and agrees with astrophysical expectations, which are believed to have an uncertainty of about $\pm 20\%$ [4,5].

Finally, we take into account the solar modulation effect, relevant only for non-relativistic $\bar{d}$: the solar wind decreases the kinetic energy T of charged cosmic rays such that the energy spectrum $d\Phi_{\bar{d}\oplus}/dT_\oplus$ of $\bar{d}$ that reach the Earth with energy $T_\oplus$ is

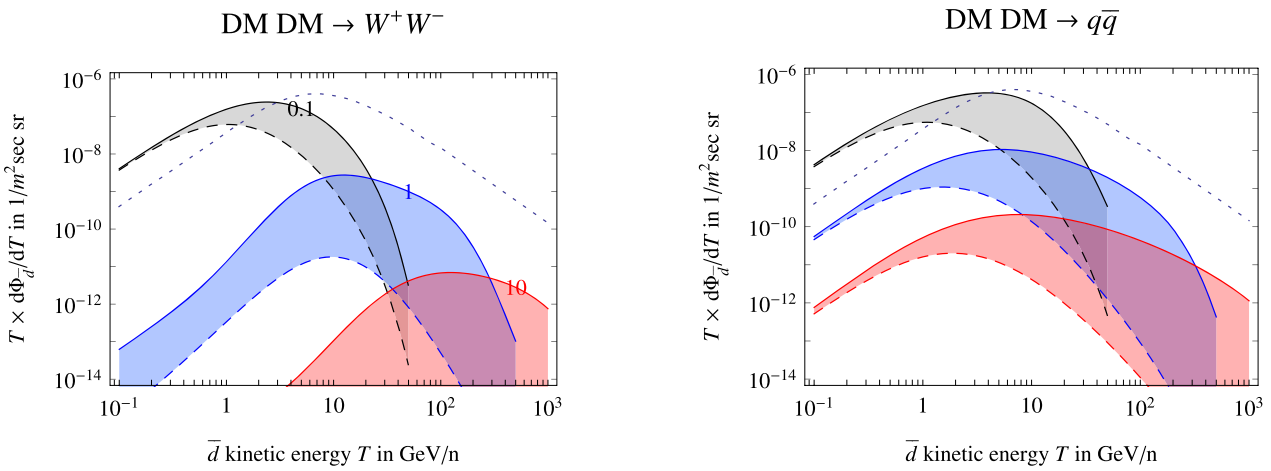

Fig. 5. Assuming the $\sigma v = 3 \times 10^{-26}$ cm^3/sec suggested by cosmology, the NFW profile, MED propagation and DM masses $M = \{0.1, 1, 10\}$ TeV, we compare the $\bar{d}$ flux obtained from the full computation (continuous lines) with the one from the spherical approximation. The dotted line is the expected astrophysical background.

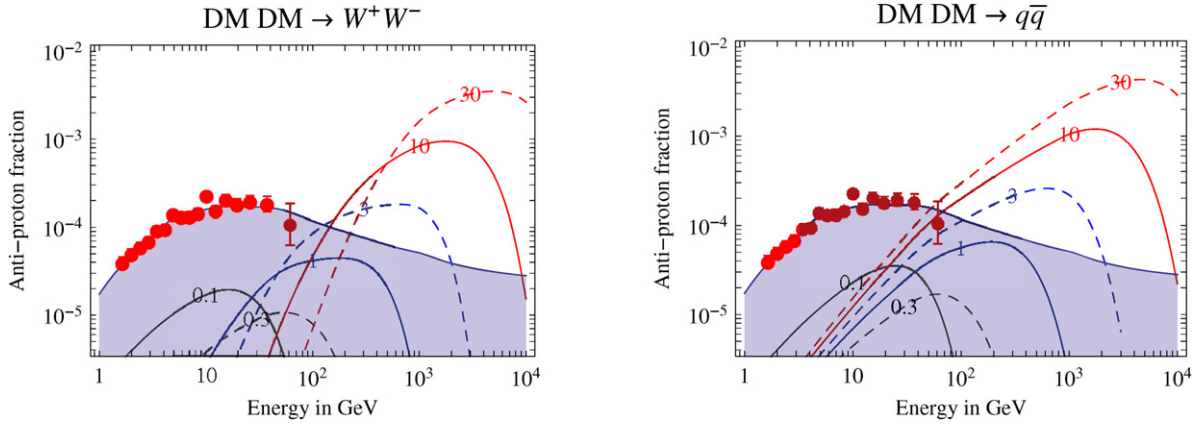

Fig. 6. The $\bar{p}/p$ ratio, for the same DM models described in the caption of Fig. 7, showing that they are compatible with the PAMELA $\bar{p}$ data (red points). Shading indicates the expected astrophysical background. (For interpretation of the references to color in this figure legend, the reader is referred to the web version of this Letter.)

approximatively related to their energy spectrum in the interstellar medium, $d\Phi_{\bar{d}}/dT$, as [17]

$$\frac{d\Phi_{\bar{d}\oplus}}{dT_\oplus} = \frac{2m_d T_\oplus + T_\oplus^2}{2m_d T + T^2}\frac{d\Phi_{\bar{d}}}{dT}, \quad T = T_\oplus + e\phi_F. \tag{12}$$

The so-called Fisk potential ϕ_F parameterizes in this effective formalism the kinetic energy loss. We assume $\phi_F = 0.5$ GV i.e. $e\phi_F = 0.5$ GeV.

4. Results

Fig. 5 compares our Monte Carlo results for the $\bar{d}$ flux with the spherical approximation.[2] The shading indicates the enhancement. We here assumed the NFW profile, MED propagation. and the DM annihilation cross section $\sigma v = \sigma v_{\text{cosmo}} \equiv 3 \times 10^{-26}$ cm^3/sec that reproduces the cosmological DM abundance via thermal freeze-out.

[2] Numerical results in some previous computations apparently included spurious factors of 2 related to dN_p/dx(after neutron decay) $\approx 2dN_p/dx$(before neutron decay) (this explains a discrepancy with [4]) and to GeV/nuc = GeV/2 (that affects the measure dT in $d\Phi_{\bar{d}}/dT$; when comparing our plots with ones in previous papers, notice that we plot $d\Phi_{\bar{d}}/d\ln T$ rather than $d\Phi_{\bar{d}}/dT$).

Rather than relying on theoretical assumptions, in order to explore the maximal $\bar{d}$ flux from DM compatible with present data, we assume

$$\sigma v = \max(1, M/300\ \text{GeV})^2 \cdot \sigma v_{\text{cosmo}}. \tag{13}$$

Indeed, Fig. 6 shows that these assumptions give a $\bar{p}$ flux compatible with (and comparable to) the PAMELA $\bar{p}/p$ data. As discussed in the previous section, the $\bar{p}/\bar{d}$ ratio is negligibly affected by astrophysical uncertainties. Furthermore, the assumed cross section is about one order of magnitude below what is needed to explain the PAMELA [18] e^+ excess and is compatible with the bounds from galactic γ and ν observations [19] as well as with the diffused γ-ray constraints [20].

Then, the upper row of Fig. 7 shows our Monte Carlo results for the $\bar{d}$ flux, $T \cdot d\Phi_{\bar{d}}/dT$, while the lower row shows the corresponding much lower $\bar{d}$ flux obtained in the spherical approximation. The caption describes all various assumptions.

Comparison of these two results shows that the signal is enhanced in our Monte Carlo $\bar{d}$ computation: almost an order of magnitude for small $\bar{d}$ kinetic energies ($T \sim 1$ GeV) or lighter DM ($M \sim 100$ GeV) and orders of magnitude at higher energies or for heavier DM. Such enhancement does not depend on the assumed value of σv. Before our calculation it was believed that only the sub-GeV energy region is suitable for searches of a DM-induced $\bar{d}$ signal. Our result implies that heavy DM, as suggested by PAMELA

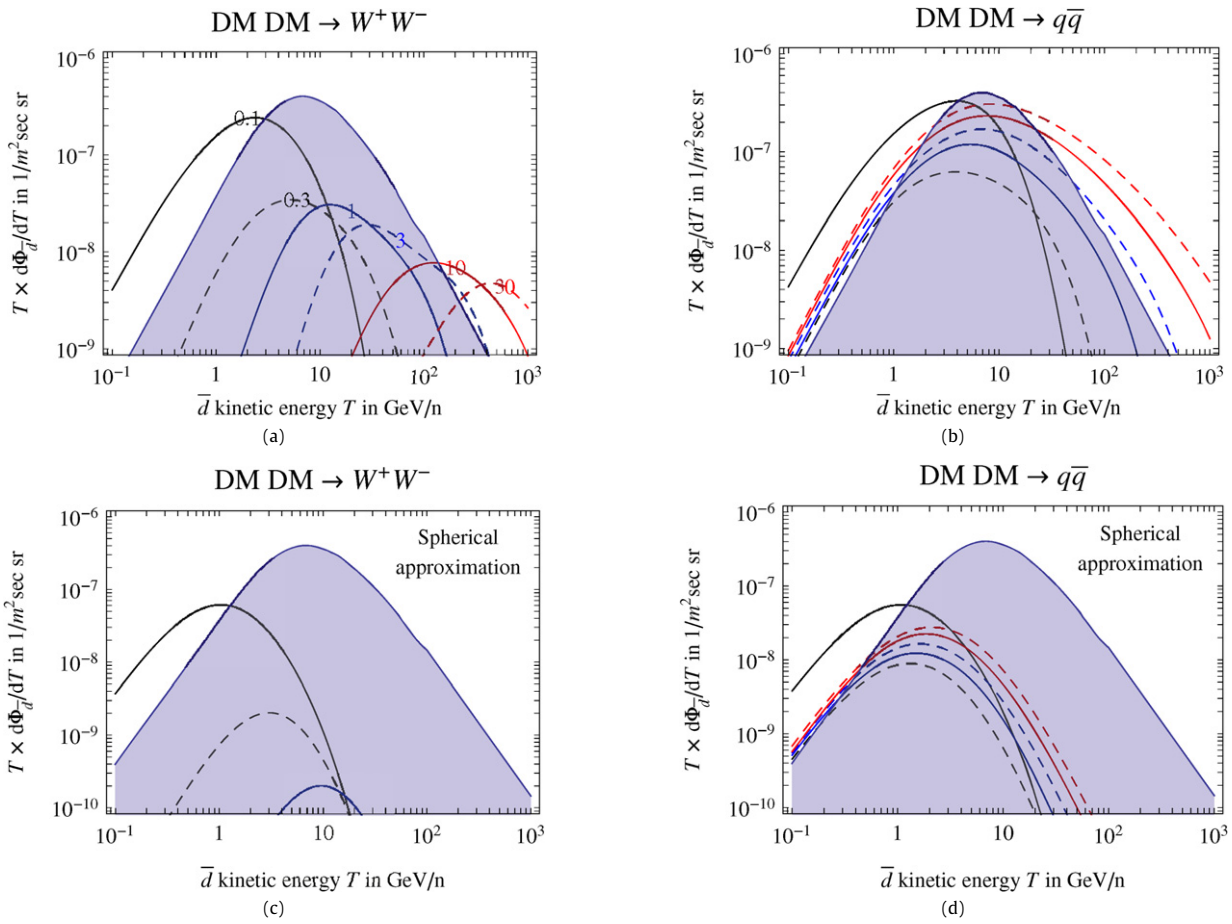

Fig. 7. Upper row: our result for the $\bar{d}$ flux at Earth. Lower row: previous results for the $\bar{d}$ flux computed in the spherical approximation. We consider DM masses $M = 0.1, 1, 10$ TeV (black, blue, red continuous curves) and $M = 0.3, 3, 30$ TeV (black, blue, red dashed curves), DM annihilations into W^+W^- (left) and $q\bar{q}$ (right) with $\sigma v = 3 \times 10^{-26}$ cm^3/sec $\times \max(1, M/300\ \text{GeV})^2$, the NFW DM profile, MED propagation, solar modulation $\phi_F = 0.5$ GV, $p_0 = 160$ MeV. Shading indicates the expected astrophysical $\bar{d}$ background. (For interpretation of the references to color in this figure legend, the reader is referred to the web version of this Letter.)

and FERMI data, also induces detectable $\bar{d}$ signal at high energies. Therefore our result has important implications on the strategy of DM searches using the $\bar{d}$ signal.

The red line in Fig. 7a roughly shows the Minimal Dark Matter [14] prediction: DM with $M \approx 10$ TeV that makes Sommerfeld-enhanced annihilations into W^+W^-, giving rise to $\bar{p}$ and consequently to $\bar{d}$ at energies (per nucleon) above $m_p M/M_W$, not yet explored by PAMELA.

The PAMELA [18], FERMI [21] and HESS [22] $e^\pm$ excesses suggest a DM interpretation in terms of multi-TeV DM that annihilates dominantly into leptons with a Sommerfeld-enhanced cross section [16,23]. An interesting class of models with these properties is obtained by assuming that DM annihilates into a new vector with mass $m < 2m_p$, that subsequently can only decay into the lighter e, μ, π [24]. We notice that this condition is not strictly necessary neither for the Sommerfeld enhancement nor for compatibility with PAMELA $\bar{p}$ data: indeed if $m \gtrsim 2m_p$ one would obtain $\bar{p}$ with energy larger than $m_p M/m$, where M/m is the boost factor of the new vector. This boost is large enough not to give an unseen $\bar{p}$ excess below 100 GeV (the energy range explored by PAMELA so far) even if m is several tens of GeV, as in [16]. Similarly to the Minimal Dark Matter case, these models would give a flux of $\bar{d}$ above 100 GeV. Our enhanced $\bar{d}$ signal should also be used to re-evaluate prospects of discovering supersymmetric Dark Matter candidates, which often annihilate into the W^+W^- or $b\bar{b}$ modes we considered.

5. Conclusions

We computed the $\bar{d}$ flux at Earth produced by DM annihilations or decays in the Milky Way using an event-by-event Monte Carlo technique run on the GRID, improving on previous computations that assumed spherically symmetric events and obtained a $1/M^2$ suppression of the $\bar{d}$ yield for heavy DM masses M. Due to the jet structure of high energy events implied by relativity no such suppression is present, and the $\bar{d}$ signal is strongly enhanced: by orders of magnitude for $\bar{d}$ energies above 10 GeV or DM masses above 1 TeV, as illustrated in Fig. 7. The $\bar{d}$ astrophysical background seems not to be significantly affected, being dominantly generated by low-energy cosmic ray collisions. While the $\bar{p}$ and $\bar{d}$ fluxes suffer from significant astrophysical uncertainties, their ratio is robustly predicted. Thereby the non-observation of a $\bar{p}$ excess in PAMELA data implies an upper bound on the $\bar{d}$ DM flux. In the light of our enhanced $\bar{d}$ fluxes, we find that a $\bar{d}$ DM signal is still possible. For example, heavy DM models [14,24] that can account for the PAMELA $e^\pm$ excess can lead to $\bar{p}$ and $\bar{d}$ excesses above 100 GeV/nucleon.

Most importantly, our result implies that the experiments searching for cosmic ray $\bar{d}$ become sensitive to $M \geqslant$ TeV mass DM, provided that the DM annihilation cross section is larger than what naively suggested by thermal freeze-out. Therefore it is important to extend future searches for $\bar{d}$ above the GeV energy range. For the moment, the AMS-2 experiment is expected to achieve a very

energy-dependent efficiency to $\bar{d}$ detection, so that AMS-2 would have a sensitivity to a $\bar{d}$ flux down to $5 \times 10^{-7}/(\mathrm{m}^2\,\mathrm{sec}\,\mathrm{sr}\,\mathrm{GeV/nuc})$ in the energy ranges 0.2 GeV/nuc $< T <$ 1 GeV/nuc (where time-of-flight is enough to discriminate $\bar{d}$ from $\bar{p}$) and 2 GeV/nuc $< T <$ 4 GeV/nuc (where the magnetic spectrometer is needed) [25]. According to previous $\bar{d}$ DM computations based on the spherically symmetric approximation, only the lower energy range was promising for DM searches. We have shown that the DM signal can manifest itself also at higher energies, where it is less affected by astrophysical uncertainties.

Acknowledgements

We thank Nicolao Fornengo, Ignazio Bombaci, Alejandro Kievsky, Torbjörn Sjöstrand, Antonello Polosa, Michele Viviani and especially Marco Cirelli for useful conversations. This work was supported by the ESF Grants 8090, 8499, Estonian Ministry of Education and Research project SF0690030s09 and by EU FP7-INFRA-2007-1.2.3 contract No. 223807.

References

[1] L.P. Csernai, J.I. Kapusta, Phys. Rep. 131 (1986) 223.
[2] F. Donato, N. Fornengo, P. Salati, Phys. Rev. D 62 (2000) 043003, arXiv:hep-ph/9904481.
[3] H. Baer, S. Profumo, JCAP 0512 (2005) 008, arXiv:astro-ph/0510722.
[4] F. Donato, N. Fornengo, D. Maurin, arXiv:0803.2640;
See also R. Duperray, et al., Phys. Lett. D 71 (2005) 083013, hep-ph/0503544;
N. Fornengo, private communication.
[5] G. Di Bernardo, C. Evoli, D. Gaggero, D. Grasso, L. Maggione, arXiv:0909.4548.
[6] C.B. Bräuninger, M. Cirelli, arXiv:0904.1165.
[7] A. Ibarra, D. Tran, arXiv:0904.1410.
[8] SphericalCow at wikipedia.
[9] ALEPH Collaboration, Phys. Lett. B 369 (2006) 192, arXiv:hep-ex/0604023.
[10] T. Sjostrand, S. Mrenna, P. Skands, Comput. Phys. Commun. 178 (2008) 852, arXiv:0710.3820.
[11] http://www.balticgrid.org.
[12] Isothermal profile: J.N. Bahcall, R.M. Soneira, Astrophys. J. Suppl. 44 (1980) 73;
NFW profile: J. Navarro, C. Frenk, S. White, Astrophys. J. 490 (1997) 493, arXiv:astro-ph/9611107;
Einasto profile: J. Einasto, Trudy Astrophys. Inst. Alma-Ata 5 (1965) 87; Tartu Astron. Obs. Teated Nr. 17;
See also: J.F. Navarro, et al., arXiv:0810.1522;
Moore profile: J. Diemand, B. Moore, J. Stadel, Mon. Not. R. Astron. Soc. 353 (2004) 624, arXiv:astro-ph/0402267.
[13] F. Donato, N. Fornengo, D. Maurin, P. Salati, Phys. Rev. D 69 (2004) 063501, arXiv:astro-ph/0306207.
[14] M. Cirelli, R. Franceschini, A. Strumia, Nucl. Phys. B 800 (2008) 204, arXiv:0802.3378.
[15] PAMELA Collaboration, arXiv:0810.4994.
[16] M. Cirelli, M. Kadastik, M. Raidal, A. Strumia, Nucl. Phys. B 813 (2009) 308, arXiv:0809.2409.
[17] L.J. Gleeson, W.I. Axford, Astrophys. J. 154 (1968) 1011.
[18] PAMELA Collaboration, arXiv:0810.4995.
[19] G. Bertone, M. Cirelli, A. Strumia, M. Taoso, JCAP 0901 (2009) 43, arXiv:0811.3744;
J. Hisano, M. Kawasaki, K. Kohri, K. Nakayama, arXiv:0812.0219 [hep-ph];
P. Meade, M. Papucci, A. Strumia, T. Volansky, arXiv:0905.0480;
J. Hisano, K. Nakayama, M.J.S. Yang, arXiv:0905.2075.
[20] G. Huetsi, A. Hektor, M. Raidal, arXiv:0906.4550 [astro-ph.CO].
[21] FERMI/LAT Collaboration, arXiv:0905.0025.
[22] H.E.S.S. Collaboration, arXiv:0811.3894;
H.E.S.S. Collaboration, arXiv:0905.0105.
[23] A. Sommerfeld, Ann. Phys. 11 (1931) 257;
J. Hisano, S. Matsumoto, M.M. Nojiri, Phys. Rev. Lett. 92 (2004) 031303, hep-ph/0307216;
M. Cirelli, A. Strumia, M. Tamburini, Nucl. Phys. B 787 (2007) 152, arXiv:0706.4071.
[24] N. Arkani-Hamed, D.P. Finkbeiner, T. Slatyer, N. Weiner, arXiv:0810.0713.
[25] V. Choutko and F. Giovacchini, Cosmic rays $\bar{d}$ sensitivity for AMS-02 experiment, talk at the ICRC07 conference.